

# Microstructural Aspects of Radiation Cured Multiacrylates

*X. Coqueret<sup>1)</sup>, B. Defoort<sup>2)</sup> and Ph. Ponsaud<sup>2)</sup>*

*<sup>1)</sup> Université de Reims Champagne Ardenne, Institut de Chimie Moléculaire de Reims  
CNRS UMR 6229, 51687 Reims Cedex, France*

*<sup>2)</sup> EADS Astrium, Avenue du Général Niox, BP 11  
33165 Saint Médard en Jalles Cedex, France*

## ABSTRACT

The radiation-induced polymerization of acrylates is known to proceed in a very heterogeneous manner and the resulting networks often display heterogeneities at various dimension scales. In particular, the early formation of microgels produces a heterogeneous structure including highly cross-linked particles together with a gelled network, with dangling chains or loops and swelling monomer. This heterogeneous character is revealed by anomalous features in the thermo-mechanical spectrum, with the broadening and the presence of shoulders in the relaxation factor ( $\tan\delta$ ) peak, but without any possibility of straightforward quantification. In order to gain an insight into the network's heterogeneity, solid state proton  $T_2$  NMR relaxation experiments were performed on radiation-cured bis-phenol A ethoxy diacrylate samples. This method allowed us to distinguish and to quantify two phases inside the materials: one phase with low mobility, and a second one with high mobility and distinct relaxation features. The decay of transverse magnetization is fitted with two components, (short or long  $T_2$ ), which can be assigned respectively to the highly and loosely cross-linked phases. The influence of acrylate conversion on the relaxation behavior of cured samples was examined. A comparison between relaxation behavior of networks obtained by UV- or by EB-induced polymerization does not reveal noticeable differences to be related to the initiation mechanism.

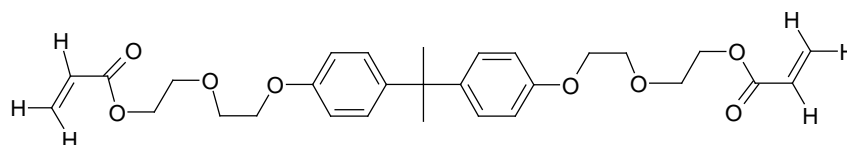
## INTRODUCTION

The electron beam-initiated polymerization of reactive prepolymer blends is now a mature technology covering the curing of fibre-reinforced composites.<sup>1</sup> The end properties of the material are controlled for a large part, by the fiber and by the matrix, separately, as well as by the fiber-matrix interface, the latter exerting usually a prime influence on the ultimate mechanical properties.<sup>2</sup> In recent years, we have examined in some details the influence of processing conditions expressed in terms of dose, dose rate, dose fractionation and thermal profiles, on the resulting network properties of the matrix.<sup>3</sup> The correlation between monomer conversion and the gradual vitrification of the network made it possible to model the kinetic profile of polymerization for curing parts of various constitution and shape under well-controlled processing conditions.<sup>4</sup> In a further step, we have focused our efforts on the micro-heterogeneity that is not taken into account by the mentioned macroscopic parameters.

Schematically, the build-up of the network by free radical polymerization of a bis-phenol A ethoxy diacrylate (Ebecryl 150) can be depicted as follows.<sup>5</sup> The polymerization starts in a liquid medium. Because of the multifunctional nature of the monomer, the cross-linking polymerization is subject to the Trommsdorff auto-acceleration effect that results from the dramatic decrease of termination rate due to the gelled environment of the propagating radicals. The polymerization then proceeds in a heterogeneous way. New “hot points” appearing in the fluid regions, whereas the microgels are gradually converted into vitrous domains in which the polymerization hardly progresses, eventually with occlusion of the propagating macroradicals. Once the percolation of the microgels is achieved, the envelope of the material is defined and it behaves as a solid. The vitrification then continues as it proceeds in uniform polymer networks subject to increasing cross-linking density.

The heterogeneous character of this type of polymerization is supported by various observations. The initially linear dependence of the volume contraction as a function of monomer conversion that levels off to reach a plateau value for conversions above 0.65 is a first peculiar behavior that will be presented in more details elsewhere.<sup>6</sup> In DMA spectra, the presence of a relaxation of smaller amplitude at a lower temperature than that of the main relaxation giving rise to the main  $\tan \delta$  peak is often interpreted in terms of acrylate networks heterogeneity.<sup>7-9</sup>

Beyond these qualitative statements, there is an obvious need for a more quantitative characterization of acrylate network heterogeneities, with a descriptor of the local mobility and the determination of the amount of material that is involved in the different domains. Solid state NMR spectroscopy is a versatile tool for characterizing polymer networks.<sup>10</sup> Litvinov et al. have successfully characterized and quantified by solid state <sup>1</sup>H NMR transverse relaxation experiments the microstructure of low  $T_g$  diacrylate networks.<sup>11</sup> We have consequently used these relaxation experiments to probe in a quantitative manner the heterogeneities induced by microgel formation in a bis-phenol A ethoxy diacrylate monomer (Scheme 1).

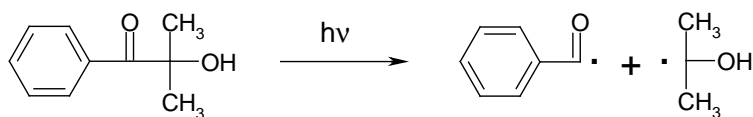


*Scheme 1 - Formula of the bis-phenol A ethoxy diacrylate monomer*

## MATERIALS AND METHODS

### Sample preparation

The difunctional monomer a bis-phenol A ethoxy diacrylate, (Ebecryl 150, UCB Radcure) was used as received, without diluents. For UV-curing experiments, 2-hydroxy 2-methyl propiophenone (Darocur 1173 - Ciba) was used as the photo-initiator at a concentration ranging from 0.1 to 0.5 wt-% (Scheme 2). The monomer was polymerized in tightly closed tubes (5 mm i.d.) or in 2 mm-deep silicone molds of dimension (6 × 70 mm<sup>2</sup>) to obtain small bars more convenient for DMA measurements. Extensive degassing in vacuo was performed to eliminate bubbles and dissolved oxygen prior to exposure to the selected radiation.



Scheme 2 - Photolysis of 2-hydroxy 2-methyl propiophenone (Darocur 1173)

## Radiation curing

Photopolymerizations were conducted under isothermal conditions by using a Linkam heating stage. The tube or the mold containing the monomer was placed inside the stage on a stand allowing good thermal contact with the heating element. The glass lid covering the stage allows efficient irradiation with a Philips TL08 UV lamp (365 nm, light intensity 1 mW/cm<sup>2</sup>). For DMA analysis, the resin was poured into a silicone mold (2×6×70 mm<sup>3</sup>) and covered with a glass plate. The samples were placed inside the stage for 3 minutes in the dark at the desired curing temperature before starting exposure to UV light. When using silicone molds, gaseous nitrogen was flushed into the stage to avoid oxygen inhibition.

The pulsed accelerator used for EB-curing was the CIRCE II generator of the Unipolis facility operating at 10 MeV. The doses were delivered in a static mode by placing the samples in front of the accelerator's hornet and by delivering the desired radiation dose. The instantaneous dose rate during the pulses of duration 12,5 μs was 530 kGy.s<sup>-1</sup>. The pulse frequency was 50 Hz and the dose was set by the overall irradiation time. Radiation doses were controlled by cellulose triacetate dosimetry.

## Conversion measurement

Double bond conversion in cured samples was determined by FTIR spectroscopy (Spectrum One FT-Spectrum Spectrometer). KBr pellets containing 1 wt-% of fine powder prepared from the cured materials were analyzed in the transmission mode. The conversion was deduced with a good accuracy from the absorbance of acrylate double bond at 810 cm<sup>-1</sup> normalized to a constant band (at 830 cm<sup>-1</sup>), as described previously.<sup>12</sup>

## DMA analysis

Dynamic mechanical analysis was performed on a DMA 2980 Dynamic Mechanical Analyzer from TA Instruments, using the dual cantilever mode, at a frequency of 1 Hz and an oscillation amplitude of 15 μm. The heating rate was 5°C.min<sup>-1</sup>.

## Proton transverse relaxation experiments

The proton T<sub>2</sub> relaxation decays were recorded on a Bruker ASX-100 spectrometer at a proton resonance frequency of 100.13 MHz, using a spin-echo pulse sequence, [(90°) - τ - (180°) - τ - FID] n, where τ varies from 6 μs to 2 ms. The intensity of the transverse magnetization is measured as a function of τ.<sup>11</sup> These relaxation experiments were performed at 20°C on powdered samples of the cured material, at a temperature far below the glass transition temperature, as revealed by the thermo-mechanical α relaxation.

## RESULTS AND DISCUSSION

The goal of this study is primarily to characterize the heterogeneity of EB-cured networks and to obtain information on the effect of processing parameters on some microstructural features of the material at various monomer conversions. Because of greater experimental simplicity and convenience, UV curing was also used to produce another series of samples allowing to compare initiation mechanisms, initiation rates and curing temperature.

### Curing conditions

It is important to stress that the two types of curing conditions were very different on two aspects of prime influence: the thermal conditions and the timescale of the treatments. UV-initiated polymerization were conducted at a low polymerization rate and with limited thermal effects, owing to the low initiator content and to the weak intensity of the light source. The slow kinetics favors isothermal conditions in the Linkam stage set at a temperature ranging from 25°C to 125°C. It also allows the production of different samples by varying the polymerization time. In contrast, EB-initiated polymerization proceeded very fast and anisothermally, a typical irradiation lasting about 100 s, when the accelerator was operated with a pulse frequency of 50 Hz.

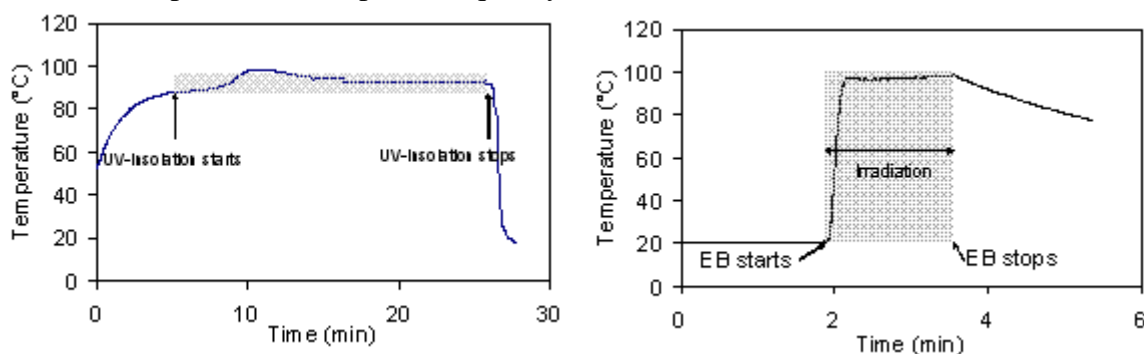


Figure 1 - Comparison of the thermal profiles for the bis phenol A ethoxy diacrylate: (left) UV-curing at 95°C for 20 min – Darocur 1173 0.4 wt-% ; (right) EB-curing with a dose of 50 kGy.

The plots shown in Figure 1 exemplify the differences in thermal profile seen by the bisphenol-A diacrylate monomer submitted to the different types of radiation-induced polymerization used in this study. Temperature measurements were recorded using a thermocouple placed in tubes containing about 10 g of monomer. For a photopolymerization experiment conducted in the Linkam stage, with external thermal regulation set at 100°C, we can see the temperature profile in the sample placed in the stage (Figure 1). UV-irradiation is started once the temperature is stabilized. A slight and temporary increase in temperature observed after 2 min of exposure is assigned to a sudden polymerization exotherm associated with the gel that is not controlled by the stage. However, the sample temperature was maintained at  $93 \pm 4^\circ\text{C}$  all along the experiment.

This is not the case during curing with EB-initiation in monomer samples initially placed at room temperature. A temperature jump of 80°C is observed immediately after the beginning of the irradiation, corresponding to the exothermal heat produced by the reaction and the energy of the electron beam. The temperature then reaches a plateau value where the released heat appears to balance the conversion of

the absorbed radiation into heat. Once the beam is stopped, heat dissipation allows the sample to cool slowly.

The utmost importance of temperature during radiation curing experiments is well-documented by reports from our group.<sup>13-15</sup> In reactive blends of interest for high performance composite materials, the progress of cross-linking polymerization is generally controlled by vitrification. Independent of the isothermal or anisothermal conditions of the polymerization, the maximum temperature of the sample on incipient vitrification will determine the level of conversion. When the mobility of active species and monomer functions is restricted in the vitrified network, a dramatic effect on propagation induces a very slow response of the material to increasing radiation dose, whatever the type initiation mechanism is.

### Thermo-mechanical properties

DMA is conveniently used to determine the glass transition temperature  $T_g$  of densely cross-linked networks. The main relaxation process is evidenced by a maximum of the damping factor  $\tan\delta$ , the maximum appearing at a temperature  $T_\alpha$  related to  $T_g$ . A typical thermo-mechanical spectrum recorded at 1 Hz in the dual cantilever mode is shown on Figure 2. It was obtained from a sample cured under UV light at 100°C for 20 min, and exhibiting a residual acrylate function content of 22 mol-%. The position of  $\tan\delta$  maximum at a temperature of 80°C would then lead to determine  $T_g$  at this temperature value. However, a shoulder is present suggesting a second relaxation maximum at ca. 0°C, which is assigned to the residual monomer and / or to networks defects, such as loops and dangling chains.

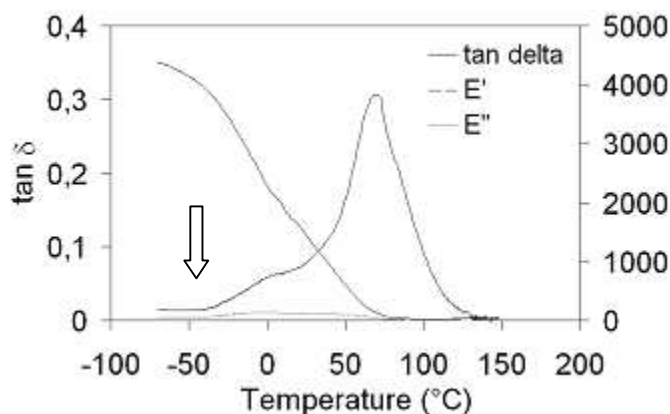


Figure 2: Temperature dependence of the storage and loss moduli  $E'$   $E''$  and loss factor measured by DMA analysis of the bis-phenol A ethoxy diacrylate UV-cured at 100°C for 20 min.

By combining  $T_g$  determination as defined above, with the measurement of monomer conversion  $\pi$  of the analyzed samples, it is worth plotting the relation  $T_g = f(\pi)$  shown in Figure 3. In the fractional conversion domain ranging from 0.5 to 0.8, the two series of values show roughly the same evolution. This result tends to prove that despite the very different thermal profiles and initiation kinetics during curing, EB- and UV-cured networks have similar macroscopic structures. It is also suggested that a single monotonous function relates the network  $T_g$  to monomer fractional conversion.

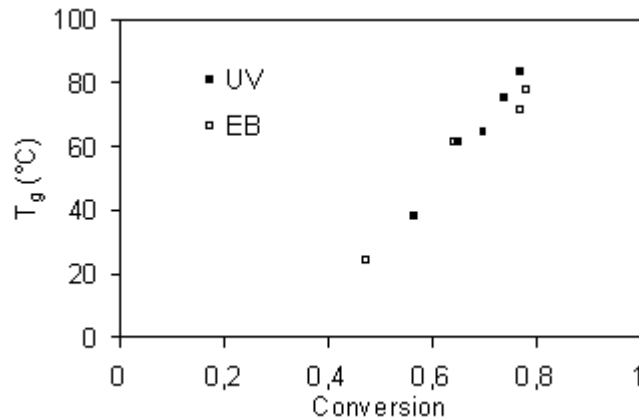


Figure 3 – Plot of the dependence of  $T_g$  on conversion for the bis-phenol A ethoxy diacrylate cured under various conditions (UV-initiation with 0.4 wt-% of Darocur 1173 or EB-curing).

The microheterogeneity of the samples is however revealed by AFM imaging. The phase contrast pictures recorded in the tapping mode revealed unambiguously a nodular microstructure with two main components of distinct modulus: some highly cross-linked particles resulting from the formation and growth of microgels tightly packed together, and some loosely or not cross-linked domain located in the confined space between the aggregates.<sup>6</sup>

### <sup>1</sup>H T<sub>2</sub> solid state NMR relaxation experiments

T<sub>2</sub> solid state NMR relaxation experiments have been successfully used by Litvinov et al. to characterize and to quantify the microstructure of low T<sub>g</sub> diacrylate networks.<sup>11</sup> The <sup>1</sup>H transverse relaxation time T<sub>2</sub> is directly sensitive to the motion of polymer chains and is thus a suitable means to investigate the network heterogeneity. If the diacrylate network can be described by percolated microgel particles with interstitial softer zones, one can try to fit the decay of magnetization by a two-component model: a cross-linked part with restricted motions (short relaxation time) and a not or loosely cross-linked part with higher mobility (longer relaxation time). The first component is assigned to the “dense network”, the second corresponding to defects such as dangling chains, loops or residual monomer trapped in the network.

The corresponding relaxation decays are generally fitted by a model consisting of a sum of exponential terms as expressed in Equation (1):

$$I(\tau)/I(0) = A + B \left\langle x \exp(-2\tau/T_{2l}) + (1-x) \exp(-(2\tau/T_{2s})^n) \right\rangle \quad (1)$$

where  $I(\tau)$  is the magnitude of the <sup>1</sup>H transverse magnetization after the time delay  $\tau$ .

There is no universal model for fitting T<sub>2</sub> relaxation decays, and various values for n can be considered. For each sample, the short T<sub>2</sub> (T<sub>2c</sub>), long T<sub>2</sub> (T<sub>2l</sub>) and the relative fraction of the two components were determined by using Equation (1). The best result was obtained with a linear combination of two single exponential functions (n=1). From these data, we can plot the gradual decrease of times T<sub>2s</sub> and T<sub>2l</sub> for increasing monomer conversion (Figure 4).

It is noteworthy that both relaxation times have similar variations regardless of the type of radiation used to induce the polymerization. Low mobility domains are observed at a fractional

conversion as low as  $\pi = 0.3$ , with a  $T_{2s}$  value of 180  $\mu\text{s}$ , decreasing to a plateau value of 15 $\mu\text{s}$  approximately reached at a fractional conversion  $\pi = 0.6$ . The  $T_{2l}$  values exhibit a larger variation, with a limiting value approaching the one determined for  $T_{2s}$  at low conversion. These variations correspond to the morphological evolution of the material, where the highly cross-linked clusters are formed at the early stage of the reaction and continue to cross-link until a maximal degree of cure. The domains rich in residual monomer are progressively converted into a denser network, as new microgel particles or as interstitial domains.

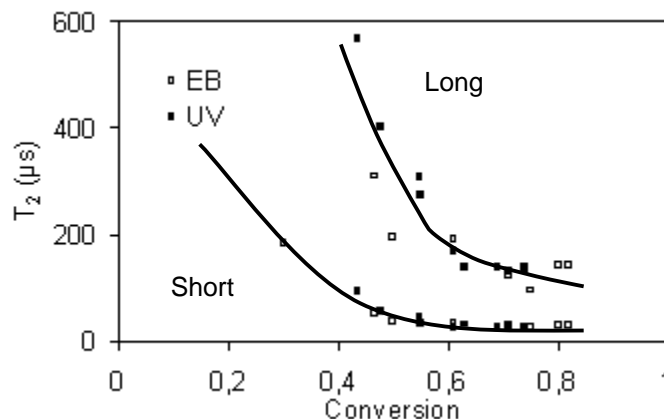


Figure 4 – Dependence of the short and long relaxation times  $T_2$  on monomer conversion in EB- and UV-cured bis-phenol A ethoxy diacrylate networks

The linear combination of exponential functions used for fitting the relaxation decays are weighted by two coefficients, directly correlated with the number of protons involved in the short and the long relaxation processes, respectively. Calling  $W_{T_{2s}} = 1 - W_{T_{2l}}$ , the coefficient associated with the short relaxation time function, we can represent the contribution of these domains with high cross-link density as a function of conversion (Figure 5). Again, independent on the type of initiation, the two series of UV- and EB-cured samples follow the same trend. These data allow us to monitor the growth of the network as a function of monomer conversion. This fraction increases up to 0.6 of conversion, where it reaches a plateau at about 85% of cross-linked fraction. It means that for the maximum conversion (about 0.82) the materials would be composed of approximately 85% of network and of 15% of unreacted monomer and defects.

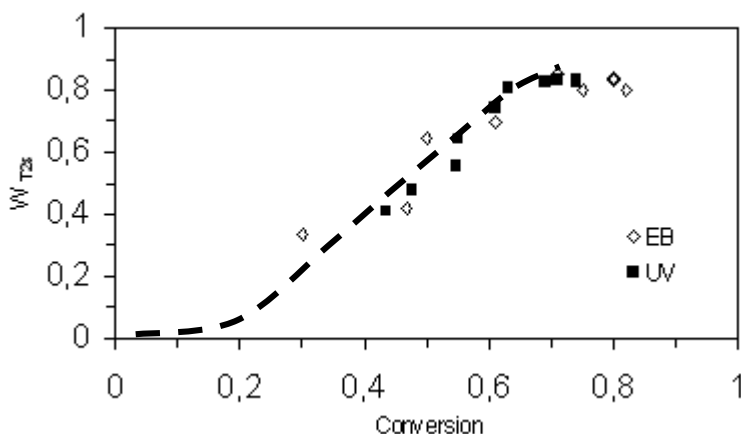


Figure 5 - Evolution of the fraction of densely cross-linked domains  $W_{T_{2s}}$  as a function of monomer conversion in EB- and UV-cured bis-phenol A ethoxy diacrylate networks.

These observations raise the issue of the influence of initiation mechanism and rate on the microstructure of the diacrylate network. With monofunctional acrylate monomers, the instant kinetic chain length is known to depend on the square root of the initiation rate, and temperature is expected to exert a dramatic effect on the occurrence of the gel effect and on occlusion<sup>6</sup>. The present results surprisingly reveal that the network structure, including its heterogeneous microstructure, have, at a given value of monomer conversion, similar features. We believe that, for this difunctional monomer, the formation of many structural defects is predominant over the kinetic factors that influence polymerization in fluid homogeneous media.

## CONCLUSION

A method based on solid state NMR relaxation measurements has been successfully used for achieving the microstructural characterization of bis-phenol A ethoxy diacrylate monomer polymerized by two different radiation, under contrasting processing conditions. This technique allowed us to characterize the heterogeneity of the materials by probing the domains of different mobility. A model with two components was shown to fit satisfactorily the relaxation decay, making it possible to quantify the local mobility by the  $T_2$  values in two types of domains, with an evaluation of their relative amount in the heterogeneous material.

It has been highlighted that EB and UV-cured networks prepared under very different kinetic and thermal conditions from bis-phenol A ethoxy diacrylate exhibit, for a given conversion level, very similar micro- and macrostructural features. Further investigation on these issues is underway in our laboratories.

## REFERENCES

- 1 - Fr. Pat. 2.564.029 Aerospatiale, inv.: D. Bézières (1984).
- 2 - B. Defoort, F. Boursereau, J. M. Dupillier, G. Larnac, G. Lopitiaux, X. Coqueret, 47th Int. SAMPE Symposium, 607 (2002).
- 3 - B. Defoort, X. Coqueret, G. Larnac, J.M. Dupillier, 45th Int. SAMPE Symposium, 2223 (2000).
- 4 - F. Boursereau, J.M. Dupillier, G. Larnac, D. Roussel, 45th Int. SAMPE Symposium, 2235 (2000).
- 5 - J. E. Elliott, C. N. Bowman, *Polymer Reaction Engineering*, 10, 1 (2002).
- 6 - P. Ponsaud, Ph.D. Dissertation, Université des Sciences et Technologies de Lille, 2005.
- 7 - K. S. Anseth, C. N. Bowman, N. A. Peppas, *Polymer Bulletin*, 31, 229 (1993).
- 8 - Y. Nakamura, M. Yamaguchi, K. Iko, *Polymer*, 31, 2066 (1990).
- 9 - A. R. Kannurpati, J. W. Anseth, C. N. Bowman, *Polymer*, 39, 2507 (1998).
- 10 - I. Ando, M. Kobayashi, M. Kanekiyo, S. Kuroki, S. Ando, S. Matsukawa, H. Kurosu, H. Yasunaga, S. Amiya, "NMR spectroscopy in polymer science" in *Experimental Methods in Polymer Science*, Wiley, New York, Chapter 4, p.261-483 (1999).
- 11 - V. M. Litvinov, A. A. Dias, *Macromolecules*, 34, 4051 (2001).
- 12 - B. Defoort, G. Larnac, X. Coqueret, *Macromol. Chem. Phys.*, 45, 3149 (2001).
- 13 - B. Defoort, D. Defoort, X. Coqueret, *Macromol. Theor. Simul.*, 9, 725 (2000).
- 14 - C. Patacz, B. Defoort, X. Coqueret, *Radiat. Phys. Chem.*, 59, 329 (2000).
- 15 - B. Defoort, G. Larnac, X. Coqueret, *Radiat. Phys. Chem.*, 62, 47 (2001).